

ANFIS-CURRENT-VOLTAGE CONTROLLED MPPT ALGORITHM FOR SOLAR POWERED BRUSHLESS DC MOTOR BASED WATER PUMP

A.Alice hepzibah A. Senthil kumar

¹Department of Electrical and Electronics Engineering, Associate Professor, Rajalakshmi Engineering College, Chennai, Tamilnadu state, India,

Email: alicehepzibah.a@rajalakshmi.edu.in

²Department of Electrical and Electronics Engineering, Professor, SKP Engineering College, Thiruvanamalai, Tamilnadu state, India,

Email: yastham@gmail.com

Abstract: *This research paper proposes to present an adaptive neuro fuzzy inference system and proportional integral controller based maximum power point tracking algorithm for solar powered brushless dc motor in order to facilitate water pumping applications. Adaptive neuro fuzzy inference with PI controller provides control gain to maximum power point tracker. It adjusts the duty cycle of the zeta converter for extracting maximum power from solar PV array. The performance of proposed controller is compared with the conventional perturb and observe method, fuzzy perturb and observe method and incremental conductance method. Simulation studies are carried out in MATLAB. The experimental verification is shown to prove the suitability and feasibility of the proposed controller. The results reveal that the adaptive fuzzy inference system with PI controller can quickly track maximum power from solar PV array under different irradiance.*

Key words: *Maximum power point tracking, ANFIS, PI controller, solar PV array*

1. Introduction

Electrical energy consumption around the world increases day by day due to huge growth in population and infrastructural changes. Hence people face huge shortage of electrical energy to meet their everyday demands [1-3]. Normally, fossil fuels are used in energy developing sectors but they are not economically viable to provide energy to consumers. Moreover they emit carbon dioxide gasses which lead to green house effect in the environment. Renewable energy sources and solar electrical energy are the feasible solutions that comply with all requirements such as no pollution and easy conversion. Solar energy can be extracted in two ways, thermal plant and solar photovoltaic cell (PV). From the existing renewable energy projects the solar PV is on the most important edge as the promising prospect of electrical energy [4-6].

The current research in solar PV is to improve the maximum power output of the PV array and it is termed as maximum power tracking techniques (MPPT). Normally, photovoltaic cell is nonlinear system i.e., current/power and voltage

characteristics have only one maximum power location. Moreover, this maximum point also varies with varying irradiance and temperature levels of the sunlight. As a result, the power inequality between sources and load characteristics restrains the accessibility of maximum power from the solar PV and it causes some major power loss in the solar electrical energy system. An electronic system used to extract the maximum power from the solar PV module to reduce the power loss is known as Maximum power point tracker. Numerous researches have been developed to extract the maximum power from the solar PV system and some literature on maximum power point algorithms are also explained in the forthcoming sections.

Perturb and observe (P&O) algorithm is the most traditional maximum power point tracking algorithm used in the solar PV array [6-9]. When compared to other MPPT algorithms, this algorithm is the simplest one which is easy to fabricate and implement. It has some disadvantages too such as tracking of maximum power being very poor during abrupt changes in irradiance and temperature. At low irradiance, oscillation occurs around maximum power point, and it leads to unstable operation of the overall solar electrical system. The response time of the algorithm is very slow with variation in irradiance level. Perturb and observe algorithm is not capable to work under noisy environment because noise factor exists in PV measurement system and it must measure critically which will otherwise tend to affect the decision making problem by the MPPT algorithm.

Currently, soft computing based maximum power point tracking algorithms such as neural network, fuzzy logic and adaptive neuro fuzzy inference system based MPPT algorithms have been developed for solar PV electrical system. The major advantages of these algorithms are that they are more stable with quick response time in all

irradiance levels at varying points. Fuzzy logic based maximum power point algorithm does not require any mathematical model for designing. But its performance depends upon the rules that are written in the fuzzy inference system. Normally these rules are created by the user i.e., human experts and hence its performance depends upon the knowledge of human experts in this field [10-11]. The designing of this algorithm is normally done through trial and error basis. The neural network based maximum point algorithm requires large amount of representative input and output data. If the data is less, then neural network does not provide optimum output for the system. Moreover, it takes more time for training due to large amount of input and output data [12-13]. Adaptive neuro fuzzy inference system based MPPT algorithm is the most accepted one because it is simple and realistic to implement and does not require large amount of input-output data. Moreover it has been implemented with significant improvement in efficiency [14].

In this paper, Adaptive neuro fuzzy inference system with PI controlled maximum power point tracking algorithms is proposed for solar water pumping system. The proposed MPPT is compared with already existing MPPT algorithm such as perturb and observe MPPT, incremental conductance MPPT, fuzzy perturb and observe MPPT. The organization of the paper is as follows: solar powered brushless dc motor for water pumping application is described in section 2. Simulation results are discussed in section 3. Experimental verification of the proposed system is presented in section 4. Concluding remarks are given in the last section.

2. Solar Powered Brushless Dc Motor for Water Pumping Application

The proposed system as shown in Fig. 1 consists of two units such as solar power conditioning unit and water pumping power conditioning unit. Solar power conditioning unit consists of solar PV panel, maximum power point tracking controllers, DC-DC zeta converter, voltage sensor, current sensor, irradiance sensor and temperature sensor. Water pumping power conditioning unit consists of electronic commutator (Voltage source PWM inverter), Brushless DC motor based water pump, hall sensor and switching pattern generator.

From figure 1, it is inferred that solar PV array electrical output is manipulated using DC-DC zeta

converter with maximum power point tracking controllers. Input for the MPPT controllers are voltage of the solar PV panel, current of the solar PV panel, irradiance level of sun light energy and temperature of the environment. Output of the MPPT controllers are PWM pulse for zeta DC-DC converter to extract maximum power from solar PV panel.

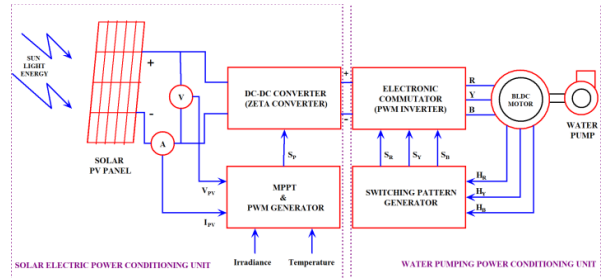


Fig.1. Solar Powered Brushless DC motor for water pumping application

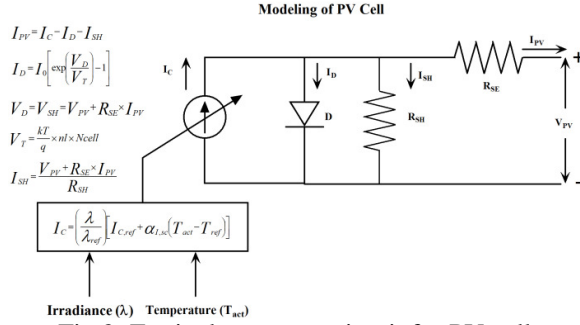
The output of the DC-DC zeta converter is fed to voltage source PWM inverter and output is fed to Brushless DC motor based water pump. Switching pulse for PWM inverter is generated based on hall sensor output and it acts as rotor position sensor for Brushless DC motor.

Solar PV panel voltage and current depends upon irradiance level of sun light and temperature level of environment. As output power level of solar PV panel decreases with decreases in irradiance level of solar light and vice versa. Normally temperature level of the environment is around 25°C to 35°C and temperature variation effect is very low in output power of the solar PV panel. If the power level of the solar PV panel varies with varying irradiance level and temperature then maximum power point tracking controller controls the duty cycle of the DC-DC zeta converter to extract maximum power from solar PV panel. The output of the DC-DC zeta converter is connected to PWM inverter. Due to variation in output voltage of the DC-DC zeta converter the speed of the Brushless DC motor varies which in turn controls the pumping level of the water pump.

A. Modeling of Solar PV array

Series and parallel string of PV cell is known as Solar PV array. The series PV cell string is used to add up the voltage level of each PV cell and parallel PV cell string is used to add up current level of each PV cell [5-6]. The equivalent power circuit of the single PV cell is shown in Figure 2.

Normally PV cell is modeled using variable current source and the magnitude current varies with irradiance level of sun light and temperature level of the environment and it is described by the following equation:



$$I_C = \left(\frac{\lambda}{\lambda_{ref}} \right) \left[I_{C,ref} + \alpha_{I,sc} (T_{act} - T_{ref}) \right] \quad (1)$$

where, λ is the irradiance level in W/m^2 , T_{act} is the temperature of the environment in Kelvin, $\alpha_{I,sc}$ is the coefficient of short circuit current and $I_{C,ref}$, T_{ref} , λ_{ref} are the standard values under standard test conditions. The PV cell consists of anti-parallel diode connected with current

source, shunt resistance and series resistance. The output current of the PV cell is expressed by the following equation:

$$I_{PV} = I_C - I_D - I_{SH} \quad (2)$$

$$I_D = I_0 \left[\exp\left(\frac{V_d}{V_T}\right) - 1 \right] \quad (3)$$

$$V_D = V_{SH} = V_{PV} + R_{SE} \times I_{PV} \quad (4)$$

$$V_T = \frac{k T_{act}}{q} \times nl \times N_{cell} \quad (5)$$

$$I_{SH} = \frac{V_{PV} + R_{SE} \times I_{PV}}{R_{SH}} \quad (6)$$

$$R_{SH} = R_{SH,ref} \times \left(\frac{\lambda_{ref}}{\lambda} \right) \quad (7)$$

$$R_{SE} = R_{SE,ref} \quad (8)$$

where, I_D is the diode current in Amps, V_D is the diode voltage in Volts, I_0 is the diode reverse

saturation current in Amps, “nl” is the diode ideality factor, k is the boltzman constant, q is the electron charge, “Ncell” is the number of cells in series in array, I_{SH} is the shunt current through shunt resistor, V_{PV} is the output voltage of the PV panel, R_{SH} is the shunt resistance in Ω , R_{SE} is the series resistance in Ω , $R_{SE,ref}$, $R_{SH,ref}$ are the standard series and shunt resistance values under standard test conditions. Considering the N_S number of series PV cell and N_P number of parallel PV cell, the modified parameter of the PV cell quantity is shown in Table 1.

Table.1. Solar PV array parameter for N_S series and N_P parallel cell

Parameters	Single PV Cell	Solar PV Array (N_S series cell and N_P parallel cell)
Light generated current	I_C	$I_C \times N_P$
Reverse saturation current	I_0	$I_0 \times N_P$
Series Resistance	R_{SE}	$R_{SE} \times \left(\frac{N_S}{N_P} \right)$
Shunt resistance	R_{SH}	$R_{SH} \times \left(\frac{N_S}{N_P} \right)$

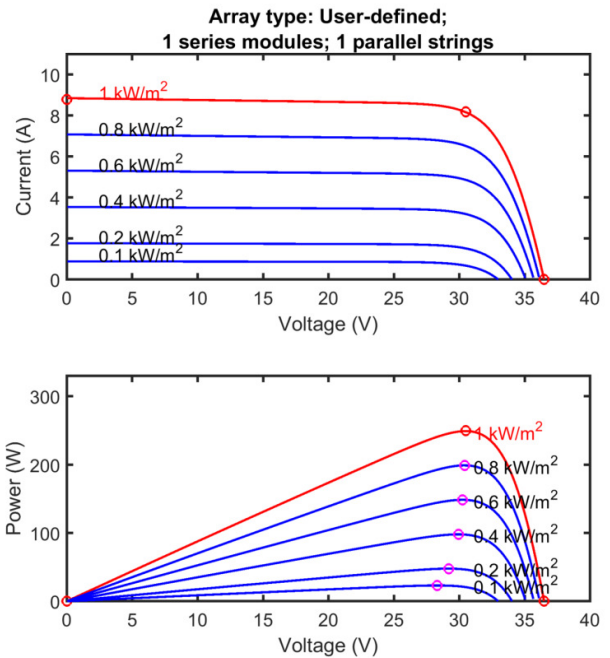


Fig.3. I-V and P-V Characteristics of single Solar PV array

The single PV cell has the following parameters such as the open circuit voltage (V_{OC}) 36.5 V, maximum power point voltage (V_{mpp}) 30.5 volts, short circuit current (I_{SC}) 8.8 A, maximum power point current (I_{mpp}) 8.2 A, maximum power point (P_{mpp}) 250 W, N_{cell} 60, light generated current (I_C) 8.8709 A, reverse saturation current (I_0) $3.2705 e^{-10}$ A, ideality factor 0.9812, shunt resistance 112.9574 Ω and series resistance 0.17045 Ω . I-V and P-V characteristics of single PV array are shown in Figure 3.

B. DC-DC zeta converter

DC-DC converters are employed as power conditioning circuit for the solar PV array with maximum power point controller to obtain the maximum power from solar PV array [11]. Normally, Buck, Boost, Buck-Boost, and Cuk converters are used as power conditioning circuit in solar PV system but these converters have some disadvantages such as when buck and boost converters are used and are operated with extreme high duty cycle, it leads to electromagnetic interference in the communication line. When Buck-Boost and cuk converters are used and output voltage is high at starting and soft starting not possible in the water pumping application with Brushless DC motor and moreover output is inverted in Buck-Boost converter. These problems can be overcome by DC-DC zeta converter. The electric circuit of DC-DC zeta converter is shown in Figure 4.

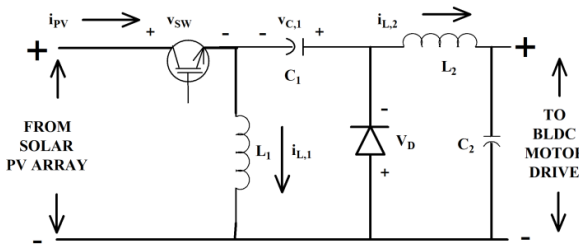


Fig.4. Electric circuit of DC-DC zeta Converter

The designed values of DC-DC zeta converters are, inductors (L_1 and L_2) 13.3 mH, capacitor (C_1) 100 μ F, DC link capacitor (C_2) 200 μ F, and switching frequency 5 kHz.

3. Adaptive Neuro Fuzzy Inference System – Proportional Integral Based Maximum Power Point Tracking controller

In this paper, adaptive neuro fuzzy inference – proportional integral controller based maximum

power point tracking controllers are proposed.

A. Adaptive Neuro Fuzzy Inference System:

ANFIS is considered to be an adaptive network, which is similar to neural networks. Adaptive network has no synaptic weights, but has so called adaptive and non-adaptive nodes. It must be said that adaptive network can be easily transformed to neural networks' architecture with classical feed forward topology [15]. ANFIS is adaptive network which works like adaptive network simulator of Takagi–Sugeno's fuzzy controllers. This adaptive network is functionally equivalent to a fuzzy inference system (FIS). Using a given input/output data set, ANFIS adjusts all the parameters using back propagation gradient descent and least squares type of method for non-linear and linear parameters, respectively. The ANFIS is composed of two parts. The first is the antecedent part and the second is the consequent part, which are connected to each other by fuzzy rules base in network form. The structure of five layers of ANFIS is shown in Figure 5.

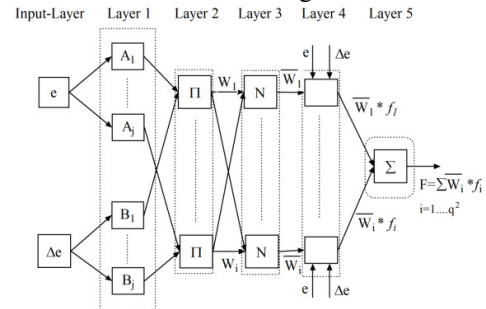


Fig.5. Structure of Five layer Adaptive Neuro Fuzzy Inference System

Layer 1: Every node i in this layer is an adaptive node with a node function which is given in equation (9) as,

$$L_{1,i} = \mu A_i(e), \text{ for } i = 1, 2 \dots j$$

$$L_{1,i} = \mu B_i(\Delta e), \text{ for } i = 1, 2 \dots j$$

(9)

Where e (or Δe) is the input node i and A_i (or B_i) is a linguistic label associated with this node. Generally Gaussian membership function is used to distribute the input variables. This function is expressed by the equation (10) as,

$$f(x; \sigma, c) = e^{-\frac{(x-c)^2}{2\sigma^2}}$$

(10)

Where c and σ represents the center and width of the membership function, parameters (c and σ) in this layer are referred to as premise parameters,

which are updated during learning process.

Layer 2: Every node in this layer is a fixed mode labeled Π , whose output is the product of all the incoming signals. Output node equation of this layer is given in (11) as,

$$L_{2,i} = W_i = \mu A_i(e) \mu B_i(\Delta e) \text{ for } i = 1, 2 \dots j^2 \quad (11)$$

Each node output represents the firing strength of a rule.

Layer 3: Every node in this layer is a fixed node labeled N. The i^{th} node calculates the ratio of the i^{th} rule's firing strength to the sum of all rules' firing strength. Node equation of this layer is given in (12) as,

$$L_{3,i} = \bar{W}_i = \frac{W_i}{\sum_{i=1}^{j^2} W_i} \quad (12)$$

Layer 4: Every node i in this layer is an adaptive node with a node function which is given in equation (13) as,

$$L_{4,i} = \bar{W}_i f_i = \bar{W}_i (p_i e + q_i \Delta e + r_i) \quad (13)$$

Where \bar{W}_i is a normalized firing strength from Layer 3 and p_i, q_i, r_i are the parameter set of this node. Parameters in this layer are referred to as consequent parameters which are updated during the learning process.

Layer 5: The single node in this layer is a fixed node labeled Σ , which computes the overall output as the summation of all incoming signals. It is represented in equation (14) as,

$$L_{5,i} = \sum_{i=1}^{j^2} \bar{W}_i f_i = \frac{\sum_{i=1}^{j^2} W_i f_i}{\sum_{i=1}^{j^2} W_i} \quad (14)$$

The premises parameter of layer 2 is updated using steepest descent method and consequent parameter of layer 4 is updated using least- squares method. Combination of these methods is known as hybrid learning of the ANFIS parameters. Hybrid learning consists of two passes namely, forward pass and backward pass. In the forward pass of the hybrid learning algorithm, nodes output go forward until layer 4 and the consequent parameters are identified by the least-square method. In the backward pass, the error signals are propagated backwards and the premise parameters are updated by gradient descent. The hybrid approach converges much faster since it reduces the search space dimensions of the original pure back propagation method.

B. Proposed ANFIS – PI controller based MPPT

Figure 6 shows the proposed ANFIS- Voltage – Current controlled and ANFIS – Voltage – Power

controlled MPPT controllers.

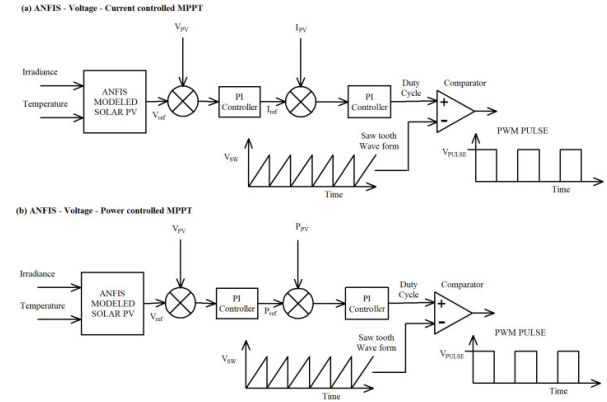


Fig.6. (a) ANFIS- Voltage- Current controlled MPPT; (b) ANFIS- Voltage- Power controlled MPPT

In this MPPT structure, duplicate model of solar PV system is modeled using ANFIS. ANFIS is trained with two inputs such as irradiance and temperature and single output such as voltage at different irradiance and temperature conditions. The output of the ANFIS system is taken as the voltage reference and is compared with actual PV voltage and produces error voltage. The error voltage is processed via Proportional Integral controller and it provides reference current and power for next stage. In the next stage, reference current or power is compared with actual PV current or PV Power and it produces error current or error power. The error current or error power is processed via Proportional Integral controller and it provides duty cycle for PWM generator. PWM generator generates the pulse for DC-DC zeta converter to extract the maximum power from solar PV array.

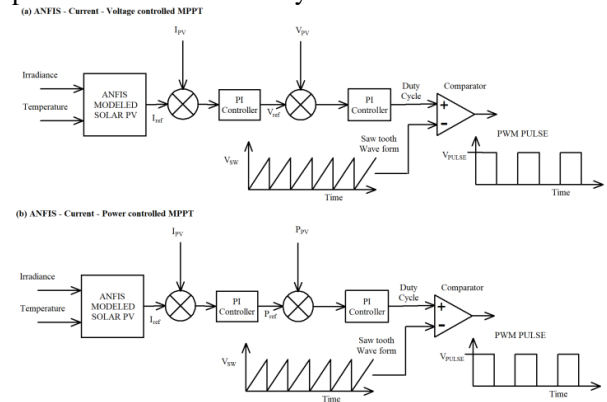


Fig.7. (a) ANFIS- Current- Voltage controlled MPPT; (b) ANFIS- Current- Power controlled MPPT

Figure 7 shows the proposed ANFIS- Current –

Voltage controlled and ANFIS – Current – Power controlled MPPT controllers. In this MPPT structure, duplicate model of solar PV system is modeled using ANFIS. ANFIS is trained with two inputs such as irradiance and temperature and single output such as current at different irradiance and temperature conditions. The output of the ANFIS system is taken as the current reference and is compared with actual PV current and produces error current. The error current is processed via Proportional Integral controller and it provides reference voltage and power for the next stage. In the next stage, reference voltage or power is compared with actual PV voltage or PV Power and it produces error voltage or error power. The error voltage or error power is processed via Proportional Integral controller and it provides duty cycle for PWM generator. PWM generator generates the pulse for DC-DC zeta converter to extract the maximum power from solar PV array.

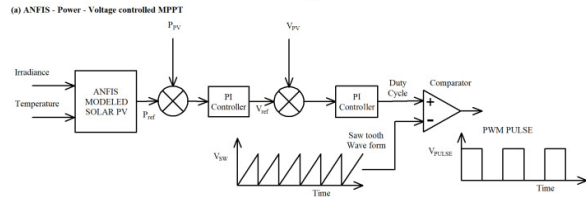


Fig.8. ANFIS- Power- Voltage controlled MPPT

Figure 8 shows the proposed ANFIS- Power – Voltage controlled MPPT controllers. In this MPPT structure, duplicate model of solar PV system is modeled using ANFIS. ANFIS is trained with two inputs such as irradiance and temperature and single output such as power at different irradiance and temperature conditions. The output of the ANFIS system is taken as the power reference and is compared with actual PV power. The error power is processed via Proportional Integral controller and it provides reference voltage for the next stage. In the next stage, reference voltage is compared with actual PV voltage and it produces error voltage. The error voltage is processed via Proportional Integral controller and it provides duty cycle for PWM generator. PWM generator generates the pulse for DC-DC zeta converter to extract the maximum power from solar PV array.

C. Brushless DC motor drive for water pumping application

Generally, voltage source pulse width modulated inverter (VSPWMI) is used to drive the Brushless DC motor. Switching logic pattern for VSPWMI is generated based on rotor position information from

the hall sensor. Six switches are used in this inverter which may be IGBT switch or MOSFET switch based on power rating of the Brushless DC motor [16]. Brushless DC motor drive for water pumping application is shown in Figure 9.

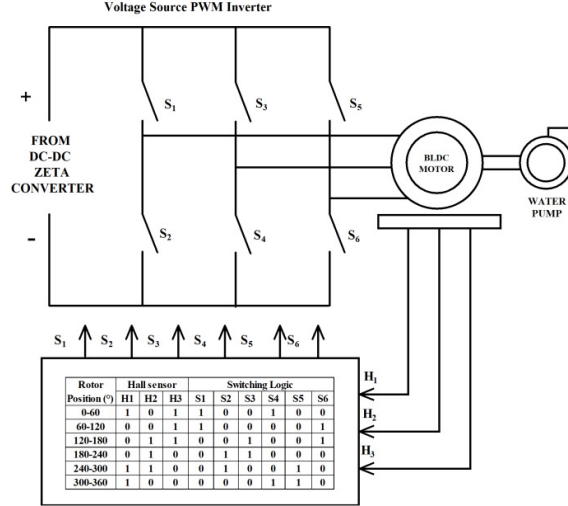


Fig.9. Brushless DC motor drive for water pumping application

4. Simulation Results and Discussions

In this section, developed simulink model is tested for varying solar irradiation level. Simulink model of solar powered brushless dc motor for water pumping application is shown in Figure 10. The simulink model consists of PV array, zeta converter, PWM inverter, brushless dc motor and MPPT controller. The parameters used in the zeta converter and brushless dc motor are shown in Table 2. The brushless dc motor is operated with hall sensor in closed loop manner.

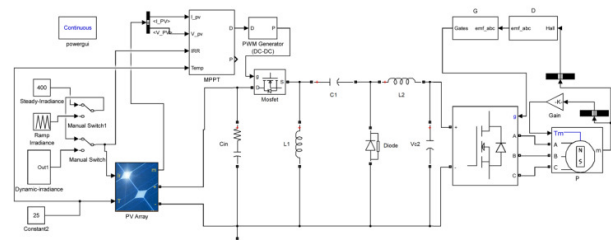


Fig.10. Simulink model of solar powered brushless dc motor for water pumping application Table.2. Parameters of zeta converter and Brushless dc motor

S.No	Zeta converter	Brushless DC motor
1	Input voltage	Rated voltage
2	Output voltage	Rated power
	Values	Values
	20~36 V	110 V
	10~100 V	200 watts

3	C_{in} and C_{out}	20000 μF	Stator phase Resistance	0.1 Ω
4	L_1 and L_2	13.3 mH	Stator phase inductance	8.5 mH
5	C_1	10000 μF	Moment of inertia	8 g-m ²
6	Switching Frequency	5 kHz	Pole pairs	2
7	Power rating	300 Watts	Torque constant	0.7 N-m/amps
8	Rated current	3 amps	Voltage constant	0.073 V/rpm

The developed simulink model is tested with nine different maximum power point tracking controllers such as perturb and observe (PO), incremental conductance (INC), perturb and observe with Fuzzy (FPO), ANFIS-Voltage control (AV), ANFIS-Voltage-Current Control (AVC), ANFIS-Voltage-Power Control (AVP), ANFIS-Current-Voltage control (ACV), ANFIS-Current-Power control (ACP) and ANFIS-Power-Voltage control (APV). The model is also tested for three different operating conditions such as steady state irradiance condition, step varying irradiance condition and ramp varying irradiance condition. In the next section, training of ANFIS controller with solar model is explained in detail.

A. Training of ANFIS controller with Solar model

In this section, ANFIS controller is trained with collected data from the PV array. Data consist of two inputs i.e., irradiance and temperature and one output i.e., PV panel voltage or PV panel current or PV panel power. The collected data are shown in Table 3.

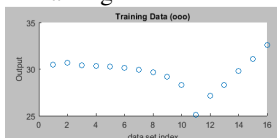
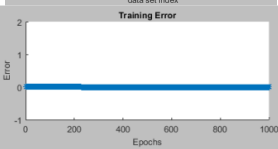

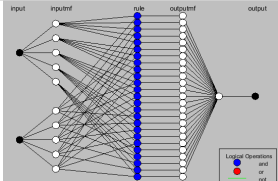
Table.3. Collected data of the PV array

S.No	Temperature (°C)	Irradiance (W/m ²)	PV voltage (V)	PV current (A)	PV Power (W)
1.	25	1000	30.50	8.21	250.1
2.	25	900	30.65	7.31	224.2
3.	25	800	30.42	6.54	199.1
4.	25	700	30.34	5.73	173.9
5.	25	600	30.26	4.91	148.6
6.	25	500	30.11	4.09	123.3
7.	25	400	29.96	3.27	98.0
8.	25	300	29.66	2.45	72.8
9.	25	200	29.21	1.63	47.8
10.	25	100	28.33	0.81	23.1
11.	25	10	25.10	0.08	002.0

12.	50	1000	27.17	8.47	230.2
13.	40	1000	28.27	8.45	239.0
14.	30	1000	29.81	8.40	250.5
15.	20	1000	31.10	8.31	258.5
16.	10	1000	32.56	8.07	262.8

Loading of input and output data of PV array is the first step in training of ANFIS controller in MATLAB. After loading of the data, membership function is defined for inputs using grid partition method or subtractive clustering method. Hybrid learning algorithm is applied to the ANFIS controller for training and 1000 iteration is being considered for training. Testing ANFIS controller with testing data is the next process. After effective testing of the ANFIS controller it is then transformed into reference PV model. Table 4 shows the training of the ANFIS controller in MATLAB.

Table.4. The training of the ANFIS controller in MATLAB

S.No	Phases of training	Phases representation of Training in MATLAB
1	Output data of the ANFIS controller	
2	Training Error Plot for 1000 iteration	
3	Testing of Trained data	
4	Structure of trained ANFIS controller	

After the training of ANFIS controller it is included in the simulink model. Figure 11 (a), (b), (c), (d), (e) shows the proposed ANFIS- PI based MPPT controller.

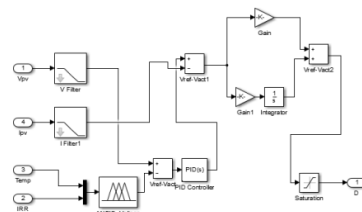


Figure 11 (a) ANFIS- Voltage- Current controlled MPPT

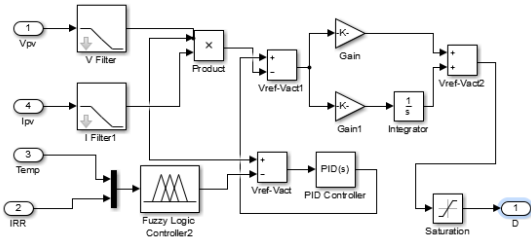


Figure 11 (b) ANFIS- Voltage- Power controlled MPPT

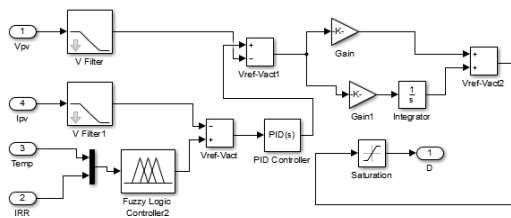


Figure 11 (c) ANFIS- Current – Voltage controlled MPPT

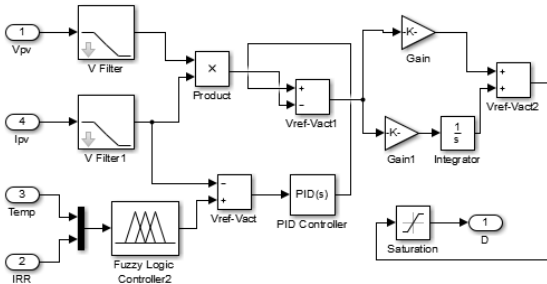


Figure 11 (d) ANFIS- Current – Power controlled MPPT

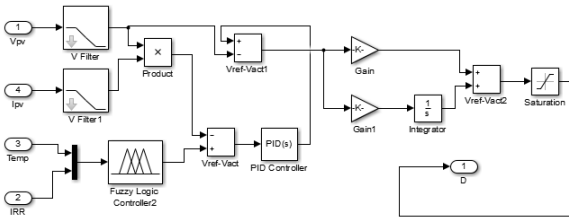


Figure 11 (e) ANFIS- Power – Voltage controlled MPPT

B. Steady state irradiation level condition

In this section, solar PV array is operated with constant irradiation of 1000 W/m^2 , 700 W/m^2 and 400 W/m^2 . Figure 12 shows the simulation results for 1000 W/m^2 , 700 W/m^2 and 400 W/m^2 .

The following results are obtained for analysis such as rise time, settling time, steady state power and steady state speed of the brushless dc motor. Performance parameters at 1000 W/m^2 , 700 W/m^2 and 400 W/m^2 are shown in Table 5, Table 6 and Table 7. From Fig.12 (a) and Table 5, ACV method have rise time of 0.15 sec and settling time of 0.19 sec but these parameters are not favourable for considered methods. The steady state power is 248 watts and steady state speed of brushless dc motor is 1270 rpm for ACV method but these parameters are not favourable for other methods.

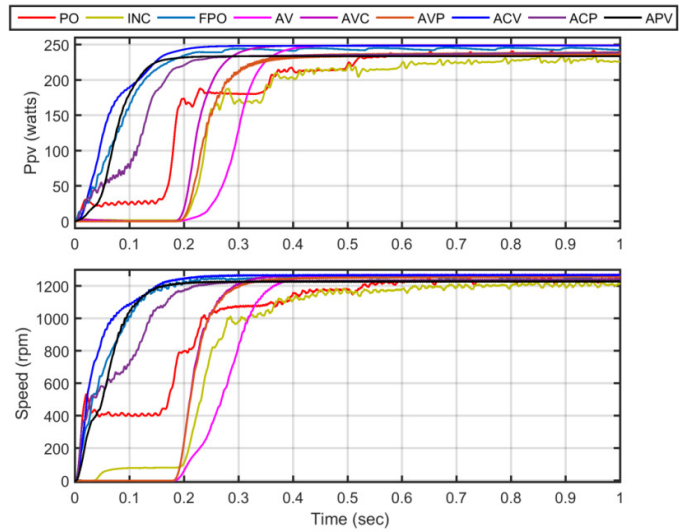


Fig.12. (a) Simulation results for 1000 W/m^2 irradiation level

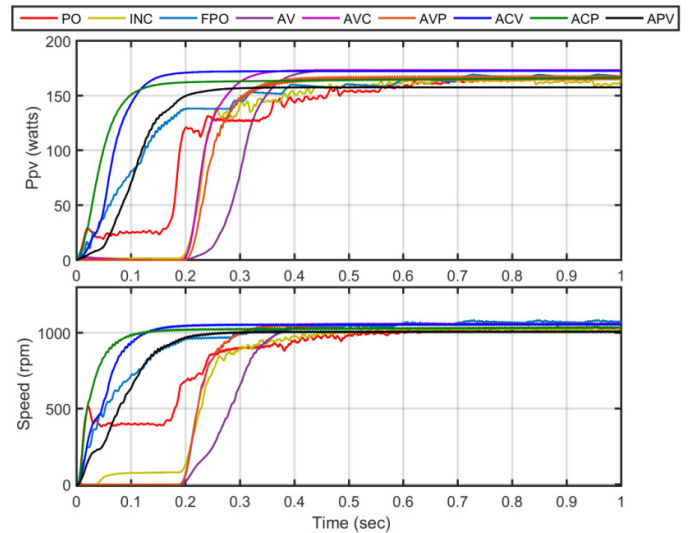


Fig.12. (b) Simulation results for 700 W/m^2 irradiation level

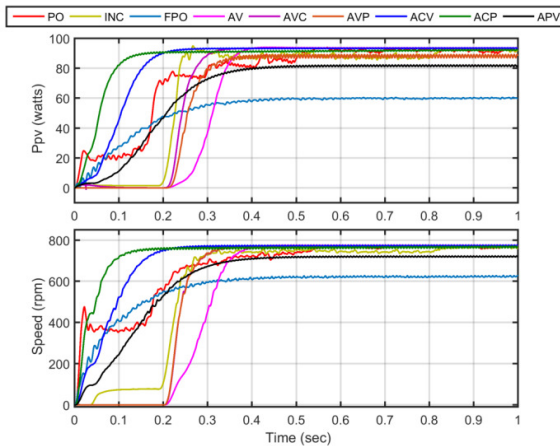


Fig.12. (c) Simulation results for 400 W/m² irradiation level

Table.5. Performance parameter at 1000 W/m²

Controller	Parameter			
	Rise time (sec)	Settling time (sec)	Power at PV array (Watts)	Steady state speed (rpm)
PO	0.5	0.59	237	1240
INC	0.6	0.69	224	1200
FPO	0.3	0.35	245	1260
AV	0.4	0.44	247	1260
AVC	0.3	0.34	247	1240
AVP	0.3	0.34	237	1260
ACV	0.15	0.19	248	1270
ACP	0.18	0.22	238	1255
APV	0.2	0.24	235	1230

Table.6. Performance parameter at 700 W/m²

Controller	Parameter			
	Rise time (sec)	Settling time (sec)	Power at PV array (Watts)	Steady state speed (rpm)
PO	0.4	0.49	162	1000
INC	0.5	0.59	162	1000
FPO	0.2	0.25	165	1025
AV	0.3	0.34	173	1075
AVC	0.2	0.24	173	1075

AVP	0.2	0.24	165	1025
ACV	0.11	0.15	174	1080
ACP	0.13	0.27	165	1025
APV	0.18	0.22	157	1003

Table.7. Performance parameter at 400 W/m²

Controller	Parameter			
	Rise time (sec)	Settling time (sec)	Power at PV array (Watts)	Steady state speed (rpm)
PO	0.35	0.41	92	772
INC	0.25	0.31	87	747
FPO	0.5	0.55	60	625
AV	0.4	0.45	93	774
AVC	0.3	0.36	93	774
AVP	0.3	0.35	87	770
ACV	0.13	0.18	94	775
ACP	0.11	0.16	92	751
APV	0.31	0.36	82	725

From Fig.12 (b) and Table 6, ACV method have rise time of 0.11 sec and settling time of 0.15 sec but these parameters are not favourable for considered methods. The steady state power is 174 watts and steady state speed of brushless dc motor is 1080 rpm for ACV method but these parameters are not favourable for other methods. From Fig.12 (c) and Table 7, ACP method have rise time of 0.11 sec and settling time of 0.16 sec but these parameters are not favourable for considered methods. The steady state power is 94 watts and steady state speed of brushless dc motor is 775 rpm for ACV method but these parameters are not favourable for other methods.

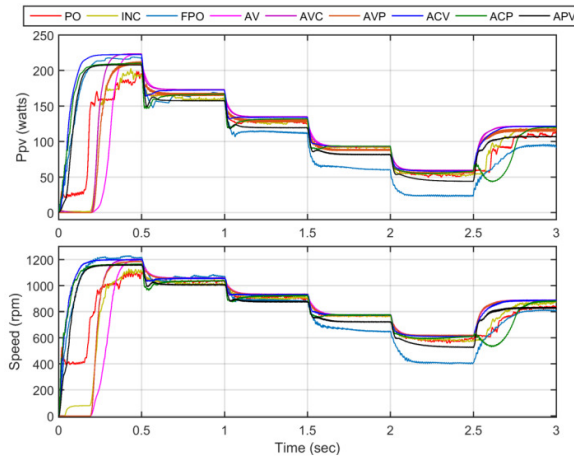


Fig.13. Simulation results for step change in irradiation level

C. Step change in irradiation level condition

In this section, solar PV array is operated with step change in irradiation level such as changing randomly at 0.5 Sec intervals, after which corresponding results are obtained for analysis. Irradiation level is changed initially from 900W/m^2 to 700W/m^2 then from 700W/m^2 to 550W/m^2 , then from 550W/m^2 to 400W/m^2 , then from 400W/m^2 to 250W/m^2 and finally from 250W/m^2 to 500W/m^2 . Figure 13 shows the results for step change in irradiance level condition. In this condition, converter output voltage and PV power is decreased and increased due to decreasing and increasing irradiation level. The speed of the brushless dc motor is decreased by decreasing irradiation level and speed is increased by increasing irradiation level. From the analysis of Figure 13, it is found that ACV method has superior tracking performance than other considered method.

D. Ramp change in irradiation level condition

In this section, solar PV array is operated with ramp change in irradiation levels such as change in linear from 100W/m^2 to 1000W/m^2 and then from 1000W/m^2 to 100W/m^2 with a time interval of 1.5 sec, after which corresponding results are obtained for analysis. Figure 14 shows the results for ramp change in irradiance level condition. In this condition too, converter output voltage and PV power is decreased linearly with decreasing irradiance level and increased linearly due to increasing irradiation level. The speed of the brushless dc motor is decreased linearly by linear decreasing irradiation level and speed is increased linearly by linear increasing irradiation level. From

the analysis of Figure 14, it is found that ACV method has superior power tracking performance than other considered methods.

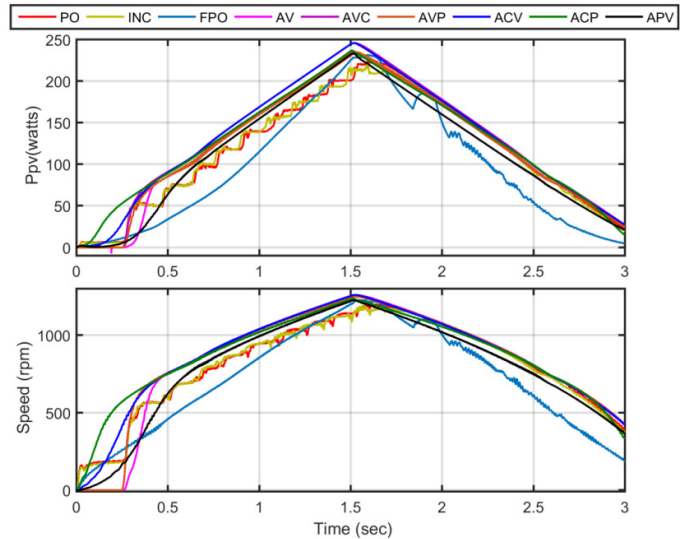


Fig.14. Simulation results for ramp change in irradiation level

From all test conditions, ANFIS-Current-Voltage controlled MPPT controller has superior performance in terms of less rise time, quick settlement and easy tracking of maximum power from PV array and maximum speed attained in the motor for all irradiance levels. It is also suitable MPPT algorithm for maximum power extraction in PV system. In the next section, experimental verification of ANFIS-Current-Voltage controlled MPPT controller for solar powered brushless dc motor for water pumping application is carried out.

5. Experimental Verification

In order to validate the proposed ANFIS-Current-Voltage controlled MPPT controller, an experimental laboratory set up is developed which is shown in Figure 15. TMS320LF2407A DSP Processor board is used to implement the proposed MPPT algorithm.



Fig.15. Experimental set up of proposed solar powered brushless dc motor based water pumping system

Time responses of the output current and voltage with proposed MPPT controller is shown in Figure 16. The zeta converter is step up with voltage up to 123.03 V for 1000 W/m², 91.66 V for 700 W/m² and 56.95 V for 400 W/m². Experimental maximum power irradiance level at 1000 W/m² is 234.9 watts, 700 W/m² is 164.98 watts and 400 W/m² is 85.99 watts. Thus the experimental results are verified with the simulation results. From the results derived, it is clear that the proposed ANFIS-Current-Voltage controlled MPPT controller performs well in all aspects for tracking maximum power from PV which will be more suitable for solar water pumping applications.

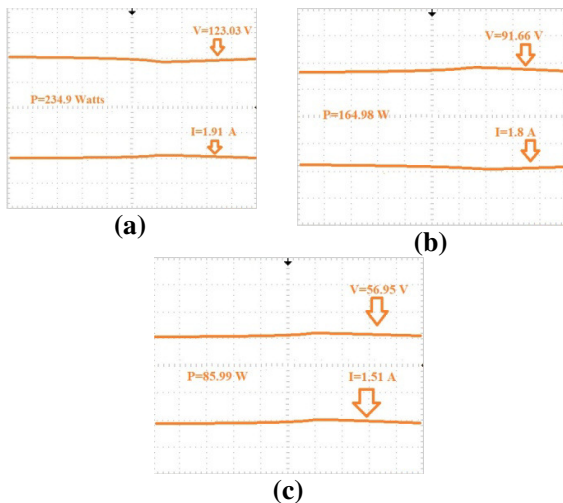


Fig.16. Time response of output voltage and current at, a) 1000 W/m², b) 700 W/m², c) 400 W/m²

Table.8. Comparison of experimental results with simulation results of ANFIS-Current-Voltage Controlled MPPT Algorithm for Solar Powered Brushless DC Motor

Irradiance level W/m ²	Based Water Pump Performance Parameter			
	Power at PV array (Watts)		Steady state speed (rpm)	
	Simulation	Experiment	Simulation	Experiment
400	94	85.99	775	710
700	174	164.98	1080	1002
1000	248	234.9	1270	1195

Simulation and experimental results of steady state irradiance level conditions match each other and corresponding performance parameters are shown in Table 8. Experimental speed values and maximum power are 7 to 9 % deviated from the performance parameters of simulation results.

6. Conclusion

A novel adaptive neuro fuzzy inference system with PI based maximum power point algorithm for solar powered brushless dc motor for water pumping application has been presented. The overall solar electrical water pumping system has been designed and simulated in MATLAB/Simulink. Effectiveness of the proposed MPPT has been analyzed and compared with conventional perturb and observe, incremental conductance and fuzzy perturb and observe MPPT. The performance of the photovoltaic system has been simulated for constant irradiance, step change irradiance and ramp change in irradiance level. The simulation results clearly show that the maximum power ratio was around 96 %, rise time response was less than 120 ms, settling time was less than 160 ms and more stable than other considered MPPT algorithm. And also the proposed MPPT was implemented with TMS320LF2407A DSP Processor and tested for 1000 W/m², 700 W/m² and 400 W/m² irradiance level. From the results, it was ascertained that, the proposed MPPT algorithm extracts maximum power from solar PV array and was closer to simulation results. Therefore, ANFIS-Current-Voltage controlled MPPT algorithm is suitable for solar water pumping application.

References

- [1] Emad Maher Natsheh., Power generation of solar PV systems in Palestine, Applied Solar Energy, 2016, Vol.52, No.3, pp.193–196.
- [2] A. T. Belenov, Yu. V. Daus, S. A. Rakitov., I. V. Yudaev, V. V. Kharchenko., The experience of operation of the solar power plant on the roof of the administrative building in the town of Kamyshin Volgograd oblast, Applied Solar Energy, 2016, Vol.52, No.2, pp.105–108.

- [3] Geury Thomas, Pinto Sonia, and Gyselinck Johan., Current source inverter-based photovoltaic system with enhanced active filtering functionalities, *IET Power Electronics*, 2015, vol.8, no.12, pp. 2483-2491.
- [4] RokeyaJahanMukti , Ariful Islam., Modeling and performance analysis of PV module with Maximum Power Point Tracking in Matlab/Simulink, *Applied Solar Energy*, 2015, Vol.51, No.4, pp.245–252.
- [5] Abdouramani Dadjé, Noël Djongyang, JanvierDomra Kana, and RenéTchinda., Maximum power point tracking methods for photovoltaic systems operating under partially shaded or rapidly variable insolation conditions: a review paper, *International Journal of Sustainable Engineering*, 2016, vol.9, no.4, pp.224-239.
- [6] Rozana Alik, Awang Jusoh, Modified Perturb and Observe (P&O) with checking algorithm under various solar irradiation, In *Solar Energy*, Volume 148, 2017, Pages 128-139.
- [7] Jirada Gosumbonggot, Maximum Power Point Tracking Method Using Perturb and Observe Algorithm for Small Scale DC Voltage Converter, In *Procedia Computer Science*, Volume 86, 2016, Pages 421-424.
- [8] RatnaIkaPutri, SptoWibowo, MuhamadRifa., Maximum Power Point Tracking for Photovoltaic Using Incremental Conductance Method, *Energy Procedia*, 2015, Vol.68, pp.22-30.
- [9] KanteVisweswara., An Investigation of Incremental Conductance based Maximum Power Point Tracking for Photovoltaic System, *Energy Procedia*, 2014, Vol.54, pp.11-20.
- [10] M. Nabipour, M. Razaz, S.GH Seifossadat, S.S. Mortazavi, A new MPPT scheme based on a novel fuzzy approach, In *Renewable and Sustainable Energy Reviews*, Volume 74, 2017, Pages 1147-1169
- [11] Saban Ozdemir, Necmi Altin, Ibrahim Sefa, Fuzzy logic based MPPT controller for high conversion ratio quadratic boost converter, In *International Journal of Hydrogen Energy*, Volume 42, Issue 28, 2017, Pages 17748-17759
- [12] Sabir Messalti, Abdelghani Harrag, Abdelhamid Loukriz, A new variable step size neural networks MPPT controller: Review, simulation and hardware implementation, In *Renewable and Sustainable Energy Reviews*, Volume 68, Part 1, 2017, Pages 221-233
- [13] Houria Boumaaraf, Abdelaziz Talha, Omar Bouhali, A three-phase NPC grid-connected inverter for photovoltaic applications using neural network MPPT, In *Renewable and Sustainable Energy Reviews*, Volume 49, 2015, Pages 1171-1179
- [14] Faiza Belhachat, Cherif Larbes, Global maximum power point tracking based on ANFIS approach for PV array configurations under partial shading conditions, In *Renewable and Sustainable Energy Reviews*, Volume 77, 2017, Pages 875-889
- [15] K. Premkumar, B.V. Manikandan., Adaptive Neuro Fuzzy Inference System based speed controller for brushless DC motor, *Neurocomputing*, 2014, Vol.138, pp.260-270.
- [16] S.A.KH. Mozaffari Niapour, S. Danyali, M.B.B. Sharifian, M.R. Feyzi, Brushless DC motor drives supplied by PV power system based on Z-source inverter and FL-IC MPPT controller, In *Energy Conversion and Management*, Volume 52, Issues 8–9, 2011, Pages 3043-3059